

## A Comparison in Hydrogen-Environment Embrittlement Response Between T6 and T73 Tempers of 7075 Aluminum Alloy

Ryo Yoshioka<sup>1</sup>, Shigeyuki Haruyama<sup>2</sup>, Ken Kaminishi<sup>2</sup>, Shuhei Osaki<sup>2</sup>

<sup>1</sup> Graduate School of Science and Engineering Yamaguchi University, Ube-shi, Yamaguchi

<sup>2</sup> Graduate School of Management of Technology Yamaguchi University, Ube-shi, Yamaguchi

(E-mail: haruyama@yamaguchi-u.ac.jp)

**Abstract** : The hydrogen-environment embrittlement (HEE) response of a high-tensile strength 7075 aluminum alloy was studied in a comparison between T6(peak-aged) and T73(overaged) tempers subjected to slow-strain rate tensile (SSRT) tests in humid air. The SSRT test (strain rate range:  $1.39 \times 10^{-4} \sim 6.95 \times 10^{-7}$  [1/s]) was carried out in 65% relative humidity air at temperatures between 10°C and 70°C in reference to an inert environment of dry nitrogen gas. With both increasing test temperature and decreasing strain rate, the alloy of T6 temper shows a more significant reduction in elongation and produces intergranular cracks in the fracture surface, resulting in a high susceptibility to HEE. In contrast, the alloy in T73 temper reveals rather an increase in elongation and transgranular dimple fracture, showing little trend of HEE. It is however found for the T73 alloy that instead of the more increase in total elongation under the lower strain rate, the uniform elongation (plastic strain until necking begins) decreases inversely. This indicates that an initiation of plastic instability is promoted by the effect of hydrogen: namely the void nucleation in grains is facilitated by hydrogen trapping at the sites of second-phase particle such as coarsened MgZn<sub>2</sub> precipitates within grains. The stop of intergranular cracking and the high resistance to HEE in the overage alloy are attributed to less diffusion of hydrogen to grain boundaries retarded by the trapping effect.

**Key words** : aluminum alloy, 7075, hydrogen embrittlement, SSRT test, temper

### 1 Introduction

The high-strength aluminum alloys can be promising materials to be applied to a high-pressure hydrogen-gas container liner or its periphery members of fuel-cell vehicles. In order to attain this, however it is necessary to ensure a safety to “hydrogen-environment embrittlement (HEE)”, which is caused by the effect of hydrogen supplied from external environments. The high-strength aluminum alloy 7075 in the peak-aged (T6) temper is well known to have usually a high susceptibility to either stress corrosion cracking or hydrogen embrittlement and thereby to result in intergranular fracture. In contrast, the overaged (T7) alloy shows a much-improved resistance and results in ductile fracture. There may be however still a limited understanding on the hydrogen effect to cause the difference in responses to embrittlement and fracture between T6 and T7 tempers. In the present study, the HEE response of a 7075 aluminum alloy plate was studied in a comparison between T6 and T73 tempers, subjected to slow-strain rate tensile (SSRT) tests in humid air, and the effect of hydrogen on the fracture process was discussed in relation to diffusion and trapping.

### 2 Experimental

#### 2.1 Material

The tested material is a high-strength alloy 7075 (Al-5.6Zn-2.5Mg-1.6Cu, mass%) rolled plate with 1 mm in thickness. The plate was subjected to the following heat treatment; solution treated for 2h at 471°C and quenched in cold water, followed by aging of T6 or T73. T6(aged for 24h at 120°C) is a temper to obtain the nearly maximum strength and T73(aged for 7h at 113°C, followed by for 10h at 178°C) is an overaged temper to improve SCC resistance. The specimen for the SSRT test is a compact smooth tensile specimen machined out in the transverse T direction perpendicular to rolling direction of plate.

#### 2.2 SSRT Test

The SSRT tests were carried out under various strain rates between  $1.39 \times 10^{-4}$  (high rate) and  $6.95 \times 10^{-7}$  (low rate) [1/s] in a humid air environment controlled to relative humidity 65% (designated as RH65%) at temperatures between 10°C and 70°C. The inert reference environment is dry nitrogen gas (designated as DNG). The susceptibility to embrittlement is estimated by using an index  $I(\delta)$  given in equation (1), indicating a reduction ratio of elongation where  $\delta$  is elongation in RH65% air and  $\delta_0$  is that in DNG.

$$I(\delta) = 1 - \frac{\delta}{\delta_0} \tag{1}$$

### 3 Results and Discussion

Figure 1 shows an example of stress-strain diagrams obtained for the peak-aged temper T6 and the overaged temper T73 subjected to the SSRT test under strain rate  $1.39 \times 10^{-6}$  [1/s] at 30°C. The T6 in RH65% air exhibits a more significant reduction in elongation compared to in DNG, resulting in an obvious embrittlement. In contrast, the T73 shows only a small reduction in elongation with little loss of tensile strength.

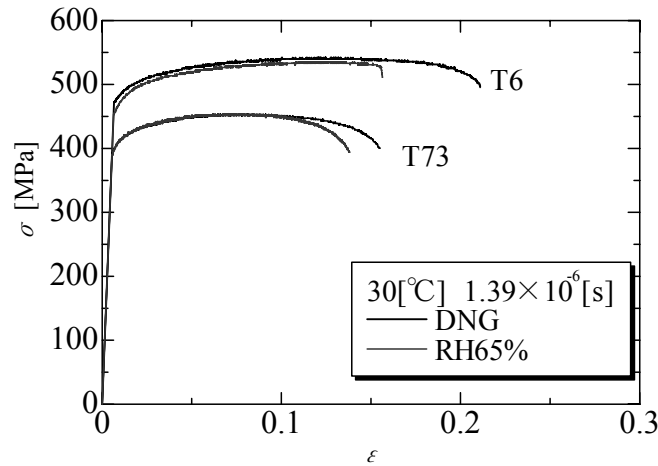


Figure 1 Stress-strain diagrams for T6 and T73 tempers of alloy 7075 SSRT-tested.

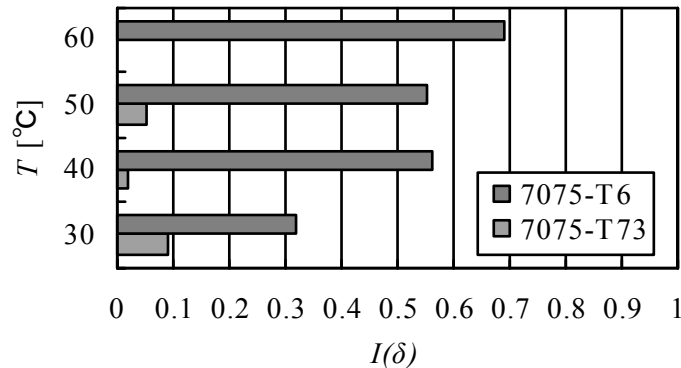
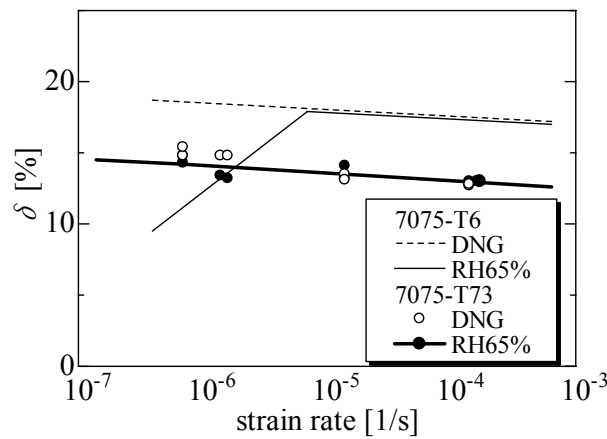


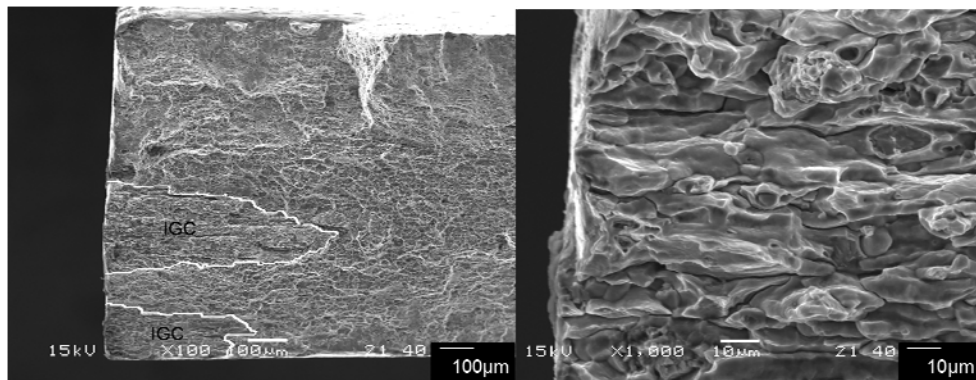
Figure 2 Comparison in index  $I(\delta)$  of susceptibility to HEE between T6 and T73 tempers.

Figure 2 illustrates  $I(\delta)$  at test temperatures between 30°C and 60°C. The T6 shows the higher susceptibility with  $I(\delta) > 0.3$  at the higher temperature, while the T73 reveals a superior resistance to HEE with  $I(\delta)$  less than 0.1 at any temperature.

Figure 3 shows the effect of strain rate on elongation to fracture  $\delta$  at 30°C for each of the T6 and the T73. With decreasing strain rate, the T6 shows rather a small increase in  $\delta$  in DNG, while in RH65% air a remarkable reduction under strain rates lower than  $6 \times 10^{-6}$  [1/s]. On a fracture surface of these specimens, an extensive intergranular crack is observed for example as shown in SEM images of Figure 4. On the other hand, the T73 in RH65% air exhibits a similar trend of increase in  $\delta$  with decreasing strain rate as in DNG, giving rise to little embrittlement ( $I(\delta) = 0.03$ ) even under a very low strain rate.



**Figure 3** The effect of strain rate on elongation to fracture  $\delta$  for T6 and T73 tempers SSRT-tested at 30°C.



**Figure 4** SEM images showing an extension of intergranular crack for the T6 temper SSRT-tested in RH65% air at 30°C under strain rate  $1.39 \times 10^{-6}$  [1/s].

Table 1 shows a detailed data on elongation together with  $I(\delta)$  for the T73 under either the high-or the low-strain rate at 30°C; total elongation  $\delta$  is composed of uniform elongation  $\delta_U$  and local elongation  $\delta_L$ , shown in a fraction as  $\delta_U/\delta$  and  $\delta_L/\delta$ , respectively. The value of  $\delta_U$  in RH65% air falls significantly compared to that in DNG, in particular to a small value ( $\delta_U=4.1\%$ ,  $\delta_U/\delta=0.28$ ) under the low-strain rate. This indicates that a necking occurs in so an earlier stage during tensile deformation, that an initiation of plastic instability would be promoted by some hydrogen effect. An increase in  $\delta_L$  ( $\delta_L=10.5\%$ ,  $\delta_L/\delta=0.72$ ) instead suggests also that hydrogen can affect the processes of void growth and coalescence until the final rupture.

**Table 1** Detailed data on elongation for the T73 temper SSRT-tested.

Strain rate[1/s]	Environment	$\delta$	$I(\delta)$	$\delta_U$	$\delta_L$	$\delta_U/\delta$	$\delta_L/\delta$
$1.39 \times 10^{-4}$ (high rate)	DNG	12.8	-	7.7	5.1	0.60	0.40
	RH65% air	13.0	-0.02	6.8	6.2	0.52	0.48
$6.94 \times 10^{-7}$ (low rate)	DNG	15.1	-	5.3	9.8	0.35	0.65
	RH65% air	14.6	0.03	4.1	10.5	0.28	0.72

SEM images showing fracture surface of the ruptured T73 specimens under the low strain rate is presented in Figure 5. The appearance of the fracture surface in each of DNG and RH65% air show a transgranular dimple fracture with bimodal dimple sizes (large and fine). An area of fine dimples is shown in the magnified images Figure 5 (b) and (d). The characteristic features in RH65% air having a larger area of fine dimple zone and a shallower depth of each dimple compared to in DNG are observed.

This suggests that the void nucleation in grains is facilitated by hydrogen effect; hydrogen trapping at the sites of second-phase particle such coarsened MgZn<sub>2</sub> precipitates within grains.

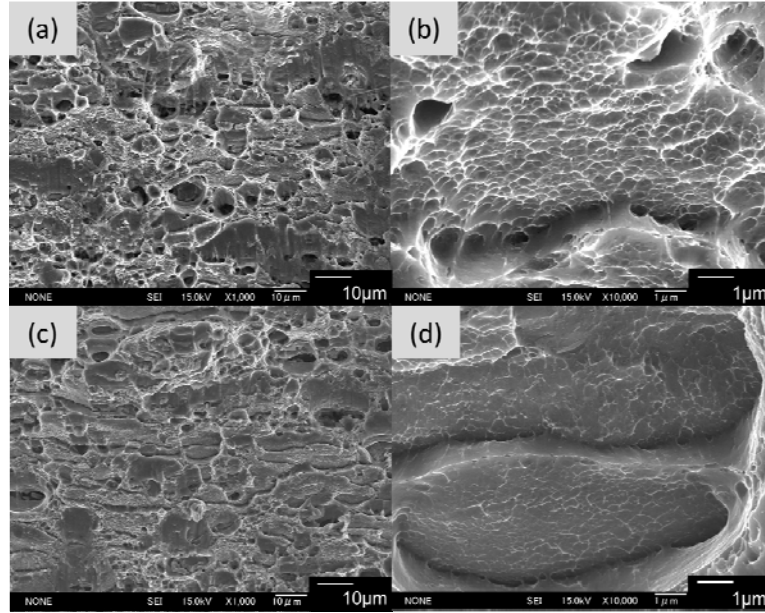


**Figure 5** SEM images showing fracture surface for the T73 temper SSRT-tested under  $6.94 \times 10^{-7}$  [1/s] at 30°C. (a),(b): DNG and (c),(d): RH65%

Using a solution of inward diffusion for a finite plate given in equation (2), it is tried to evaluate a surface profile of hydrogen concentration, where  $C_x$  is a hydrogen concentration at depth  $x$  from specimen surface,  $C_s$ : surface concentration,  $t_i(P)$ : time required for plastic strain to maximum stress in SSRT testing and  $D_{eff}$ : effective diffusion coefficient including trapping effect, given by equation (3).

$$\beta = \frac{c_x}{c_s} = 1 - \frac{4}{\pi} \sum_{\nu=0}^{\infty} \frac{1}{2\nu+1} \sin \left[ \frac{(2\nu+1)\pi x}{d} \right] \exp \left[ - \frac{(2\nu+1)^2 \pi^2 D_{eff} t_i(P)}{d^2} \right] \quad (2)$$

$$D_{eff} = D_0 \exp \left( - \frac{Q}{RT} \right) \quad (3)$$

Provided that activation energy  $Q$  is 16.4[kJ/mol] for the T6<sup>[1]</sup> and 32[kJ/mol] for the T73<sup>[2]</sup>,  $D_{eff}$  is given as listed in **Table 2** when  $D_0 = 1.68 \times 10^{-10}$  [m<sup>2</sup>/s]<sup>[3]</sup>. Using  $t_i(P)$  measured in the SSRT tests which implies an initiation time of intergranular cracking for the T6,  $\beta$  at a critical depth  $x = 16$  [μm], equal to twice of grain diameter is calculated. Obtained values of  $\beta$  are 0.93 for the T6 and 0.38 for the T73, respectively. Diffusivity of the T73 is so more decreased than that of the T6 due to a hydrogen trapping effect by coarsened precipitates within grains, leading to insufficient hydrogen concentration to cause intergranular cracks. Instead, however, an increase in local elongation can be resulted from the enhanced nucleation of micro-voids at the trapping sites and subsequent voids growth and coalescence.

**Table 2** Summary of activation energy  $Q$ , effective diffusivity  $D_{eff}$  and hydrogen concentration ratio  $\beta$  for the T6 and T73 tempers.

Temper	T6	T73
$Q$ [kJ/mol]	16.4	32
$D_{eff}$ [m <sup>2</sup> /s]	$2.5 \times 10^{-13}$	$5.1 \times 10^{-16}$
$\beta$	0.929	0.380

#### 4 Summery

The hydrogen-environment embrittlement (HEE) response of a high-tensile strength 7075 aluminum alloy plate was studied in a comparison between T6 (peak-aged) and T73 (overaged) tempers, subjected to slow-strain rate tensile (SSRT) tests in humid air. The obtained results are summarized as follows.

- (1) With both increasing test temperature and decreasing strain rate, the T6 temper shows a more significant reduction in elongation and produces intergranular cracks in the fracture surface, resulting in a high susceptibility to HEE. In contrast, the T73 temper reveals rather an increase in elongation and transgranular dimple fracture, showing little trend of HEE.
- (2) It is found for the T73 temper that a uniform elongation (a part of total elongation until necking begins) in humid air decreases than that in dry nitrogen gas. This implies that an initiation of plastic instability is promoted by hydrogen effect: namely suggesting that the void nucleation in grains is facilitated by hydrogen trapping at the sites of second-phase particle such coarsened  $MgZn_2$  precipitates within grains.
- (3) The stop of intergranular cracking and the high resistance to HEE in the T73 temper are attributed to less diffusion of hydrogen to grain boundaries retarded by the trapping effect.

### **Reference**

- [1] Y.Nakashima, S.Haruyama and S.Osaki: Proc. 119 Forum of Japan Inst. Light Metals, JILM, (2010), 321-322
- [2] G.A.Young and J.R.Scully: Hydrogen effects on material behavior and corrosion deformation interactions, Ed, N.R.Moody, at al, TMS, (2003), 893-907
- [3] R.J.Gest and A.R.Troiano: Corrosion, 30(1974), 274-279